



**HAL**  
open science

# Population viability analysis of plant and animal populations with stochastic integral projection models

Malo Jaffré, Jean-François Le Galliard

► **To cite this version:**

Malo Jaffré, Jean-François Le Galliard. Population viability analysis of plant and animal populations with stochastic integral projection models. *Oecologia*, 2016, 10.1007/s00442-016-3704-4. hal-01366598

**HAL Id: hal-01366598**

**<https://hal.sorbonne-universite.fr/hal-01366598>**

Submitted on 14 Sep 2016

**HAL** is a multi-disciplinary open access archive for the deposit and dissemination of scientific research documents, whether they are published or not. The documents may come from teaching and research institutions in France or abroad, or from public or private research centers.

L'archive ouverte pluridisciplinaire **HAL**, est destinée au dépôt et à la diffusion de documents scientifiques de niveau recherche, publiés ou non, émanant des établissements d'enseignement et de recherche français ou étrangers, des laboratoires publics ou privés.

1 **Population viability analysis of plant and animal populations with**  
2 **stochastic integral projection models**

3

4 Malo Jaffré <sup>1,2</sup> and Jean-François Le Galliard <sup>2,3</sup> \*

5

6 1. Département de Biologie, École Normale Supérieure, 46 rue d'Ulm, 75005 Paris, France.

7 2. CNRS, UMR 7618, iEES Paris, Université Pierre et Marie Curie, Case 237, 7 Quai St

8 Bernard, 75005 Paris, France.

9 3. CNRS, UMS 3194, CEREEP - Ecotron Ile De France, École Normale Supérieure, 78 rue

10 du Chateau, 77140 St-Pierre-lès-Nemours, France.

11

12 \* Correspondence author:

13 CNRS - UMR 7618, iEES Paris, Université Pierre et Marie Curie

14 Case 237, Bâtiment A, 7 Quai St Bernard

15 75005 Paris, FRANCE

16 Phone: +33.1.44.27.26.68

17 Email: galliard@biologie.ens.fr

18

19 **Author Contributions:** MJ and JFLG conceived and designed the study. MJ and JFLG

20 designed the models and JFLG provided data. MJ performed all analyses. MJ and JFLG wrote

21 the manuscript.

22

23

24 **Abstract**

25 Integral projection models (IPM) make it possible to study populations structured by  
26 continuous traits. Recently, Vindenes *et al.* (2011) proposed an extended IPM to analyse the  
27 dynamics of small populations in stochastic environments, but this model has not yet been  
28 used to conduct population viability analyses. Here, we used the extended IPM to analyse the  
29 stochastic dynamics of IPM of small size-structured populations in one plant and one animal  
30 species (evening primrose and common lizard) including demographic stochasticity in both  
31 cases and environmental stochasticity in the lizard model. We also tested the accuracy of a  
32 diffusion approximation of the IPM for the two empirical systems. In both species, the  
33 elasticity for  $\lambda$  was higher with respect to parameters linked to body growth and  
34 size-dependent reproduction rather than survival. An analytical approach made it possible to  
35 quantify demographic and environmental variance in order to calculate the average stochastic  
36 growth rate. Demographic variance was further decomposed to gain insights into the most  
37 important size classes and demographic components. A diffusion approximation provided a  
38 remarkable fit to the stochastic dynamics and cumulative extinction risk, except for very small  
39 populations where stochastic growth rate was biased upward or downward depending on the  
40 model. These results confirm that the extended IPM provides a powerful tool to assess the  
41 conservation status and compare the stochastic demography of size-structured species, but  
42 should be complemented with individual based models to obtain unbiased estimates for very  
43 small populations of conservation concern.

44

45 **Keywords:** extinction, life cycle, population viability analysis, trait-based approach.

46

47

48 **Introduction**

49 Ecological impacts of human activities have altogether caused a massive loss of species  
50 (Hughes et al. 1997), and the abundance of many species has crossed a critical threshold for  
51 the population viability (Gilpin and Soulé 1986). Therefore, a better understanding of small  
52 population dynamics should give crucial insights to predict, and where possible remedy,  
53 extinction. Population dynamics results from an interplay between deterministic components,  
54 stochastic components, and the life history (Benton et al. 2006; Lande et al. 2003). For  
55 example, populations of common lizards are regulated by density dependent feedbacks (i.e.,  
56 deterministic component) and also fluctuate due to yearly changes in weather conditions (i.e.,  
57 random component, Le Galliard et al. 2010). Given that importance of stochastic factors in  
58 small populations, one major topic in conservation biology is to evaluate how random,  
59 demographic variation affects population viability across diverse life histories (Beissinger and  
60 McCullough 2002; Morris and Doak 2002). Demographic variation can be explained by  
61 random fluctuations in climate, resource availability, and other extrinsic factors that generate  
62 simultaneous changes among individuals at a given time (i.e., environmental stochasticity).  
63 Demographic variation can also be explained by random inter-individual differences (i.e.,  
64 demographic stochasticity), non-random differences among individuals (e.g., differences in  
65 quality at birth) and sampling effects (Kendall and Fox 2002).

66 Models to describe stochastic dynamics and calculate extinction risk for small  
67 populations often hypothesise a discrete time process and a discrete stage structure  
68 (Beissinger and McCullough 2002; Caswell 2001; Morris and Doak 2002). They rely on a  
69 projection matrix whose entries are transition rates within and between stages (e.g., survival  
70 and reproduction in an age structured population, Caswell 2001). Such matrix projection  
71 models (MPM) make it possible to include, for example, effects of environmental (Lande and  
72 Orzack 1988; Tuljapurkar 1990) and demographic stochasticity (Engen et al. 2005). Thus,

73 most population viability analyses (PVA) are based on MPM for which robust protocols have  
74 been defined to assess conservation status, make demographic projections and test alternative  
75 management scenarios (Morris and Doak 2002). However, the life history of many species is  
76 often characterised by a life history structure that depends on continuous traits, sometimes in  
77 conjunction with a discrete stage structure (Benton et al. 2006; Ellner and Rees 2006). For  
78 example, size (or height in plants) are key determinants of demographic variation in natural  
79 populations of snakes and lizards (Baron et al. 2013; Le Galliard et al. 2010), and many  
80 species of mammals, birds and plants (Merow et al. 2014).

81         Continuously structured life histories can be modelled with a large transition matrix  
82 made out of numerous classes and the demographic parameters in a MPM can be estimated  
83 from regression on continuous traits (Gross et al. 2006). In such cases, however, the use of  
84 MPM may come at the cost of precision of model parameters, generate difficulties of  
85 numerical implementation in small data sets, and induce potential changes in the ranking of  
86 sensitivities (Easterling et al. 2000; Enright et al. 1995; Pfister and Stevens 2003). Instead,  
87 Easterling *et al.* (2000) and Ellner and Rees (2006) recommended to use regression  
88 techniques to estimate demographic traits in an integral projection model (IPM). Ramula *et al.*  
89 (2009) further demonstrated that the IPM can outperform the MPM for small data sets  
90 because the IPM estimates the asymptotic growth rate  $\lambda$  with less bias and variance. In a  
91 recent study, Vindenes *et al.* (2011) proposed an extended IPM to model continuously  
92 structured life histories for small populations in fluctuating environments. This extension of  
93 IPM theory assumes small demographic fluctuations (i.e., small noise approximation) and  
94 allows to approximate population dynamics by a diffusion process. The new mathematical  
95 framework of Vindenes *et al.* (2011) should provide a useful addition to the PVA toolbox in  
96 conservation biology because it allows to model size-structured stochastic population  
97 dynamics. However, to our knowledge, this new framework has never been applied in real life

98 situations and the accuracy of the small noise approximation have not been thoroughly  
99 investigated.

100         In this study, we used the newly developed, extended IPM and tested the accuracy of  
101 the diffusion approximation for two particular empirical systems. First, we applied the  
102 extended IPM to the case of two natural populations, including (i) a widespread monocarpic  
103 perennial plant species (redsepal evening primrose, *Oenothera glazioviana*) previously  
104 studied with a deterministic IPM (Rees and Rose 2002), and (ii) a widespread lizard species  
105 (common lizard, *Zootoca vivipara*) characterised by a strong size structure and temporal  
106 fluctuations in survival (Le Galliard et al. 2010). We chose these two study systems because  
107 they represent an increasing complexity from a system influenced solely by demographic  
108 stochasticity to a system influenced by the combined action of demographic and  
109 environmental stochasticity. In addition, the primrose represents a natural situation with a  
110 positive deterministic growth, which is encountered in some reintroduction programs in  
111 conservation biology (Beissinger and McCullough 2002; Morris and Doak 2002). On the  
112 contrary, the lizard represents a natural situation with a negative growth typical of the study of  
113 endangered, declining species. Thus, these two examples are useful testbeds to demonstrate  
114 the flexibility of the extended IPM for conservation biology. In each case study, we used the  
115 extended IPM to conduct a standard PVA including the calculation and decomposition of the  
116 stochastic population growth rate, the analysis of demographic stochasticity, and the  
117 simulation of extinction dynamics. We compared outcomes of this PVA with those of an  
118 individual based, simulation version of the IPM. Second, we also quantified the accuracy of  
119 the diffusion approximation in numerous, alternative parameterisations of the primrose model  
120 ranging from positive to negative growth and from low to very high values of demographic  
121 variance. We did so to investigate more thoroughly the accuracy of the diffusion  
122 approximation without confounding effects of differences in life history structure between the

123 two species.

124 **Materials and methods**

125 **Integral projection model**

126 Let's assume that the life history is structured by one continuous variable called  $y$  such that  
 127 individuals differ by  $y$  only and  $y$  is a major determinant of vital rates; for example  $y$  could  
 128 correspond to body size in animal or height in a plant. The population can then be described  
 129 by the probability density of individual size  $y$  at time  $t$ , defined by the continuous function  
 130  $n(y,t)$ , such that  $n(y,t)dy$  is the number of individuals between trait values  $y$  and  $y+dy$   
 131 at time  $t$  (Easterling et al. 2000). Total population size at time  $t$  is called  $n(t) = \int_{\Omega} n(y,t)dy$ ,  
 132 where  $\Omega$  is the domain of possible values for trait  $y$ . The general structure of the  
 133 time-invariant IPM of a large population writes like:

134 
$$n(y,t+1) = \int_{\Omega} k(y,x)n(x,t)dx = \int_{\Omega} [s(x)f_s(y,x) + b(x)f_b(y,x)]n(x,t)dx \quad (1)$$

135 where  $k(y,x)$  is the kernel describing transition rates from state  $x$  at time  $t$  to state  $y$  at time  
 136  $t+1$ . According to equation (1), the kernel can be further decomposed into (1) the  
 137 survival-growth kernel where  $s(x)$  is the survival probability of an individual with trait value  
 138  $x$ , and  $f_s(y,x)dy$  is the probability of reaching trait value between  $y$  and  $y+dy$  at time  
 139  $t+1$  for an individual of trait value  $x$ , and (2) the fecundity kernel where  $b(x)$  is the fecundity  
 140 of an individual with trait value  $x$ , and  $f_b(y,x)$  is the probability density function of the trait  
 141 value of offspring. This deterministic IPM can be considered as a matrix projection model  
 142 (MPM) with an infinite number of discrete classes. Thus, according to the seminal paper by  
 143 Easterling *et al.* (2000), most of the properties of MPM can be generalised to IPM, including  
 144 the calculation of the deterministic population growth rate  $\lambda$ , the determination of  
 145 equilibrium population structure  $u(y)$  and reproductive values  $v(y)$  and the calculation of

146 deterministic elasticities of  $\lambda$ . Here, we used a numerical method to simulate IPM by  
 147 discretising the state-space  $\Omega$  into  $C$  classes of the same width and computing integrals  
 148 using Simpson's 3/8 method, a more accurate numerical integration method than the standard  
 149 mid-point rule (Merow et al. 2014). A spectral analysis of this discretised IPM allows to  
 150 determine the dominant eigenvalue (called  $\lambda$ ), the right eigenvector  $u(x)$  scaled so that  
 151  $\int_{\Omega} u(x)dx = 1$ , and the left eigenvector  $v(x)$  scaled so that  $\int_{\Omega} v(x)u(x)dx = 1$ . The right  
 152 eigenvector corresponds to the stable trait distribution, while the left eigenvector corresponds  
 153 to the reproductive value distribution, which measures the contribution of an individual to  
 154 future population growth relative to other individuals in the population.

### 155 **Finite population in a stochastic environment**

156 To describe the dynamics of a small population in a fluctuating environment, we introduce the  
 157 stochastic IPM:

$$158 \quad N(y, t+1) = \int_{\Omega} K(y, x, Z_t) N(x, t) dx, \quad (2)$$

$$159 \quad K(y, x, Z_t) = s(x, Z_t) f_s(y, x, Z_t) + b(x, Z_t) f_b(y, x, Z_t)$$

160 where  $N$  is the discrete population size,  $K$  is a stochastic kernel, and  $Z_t$  is a random  
 161 vector describing parameter values at time  $t$  and thus the environmental state. The model  
 162 described by equation (2) is similar to the deterministic model of equation (1) conditional on  
 163  $Z_t$ . Here, we consider that  $Z_t$  is a vector of year-specific parameters and assumed that  
 164 parameter values vary randomly over time according to the random effects model of Rees and  
 165 Ellner (2009). This implies that elements of the stochastic kernel of the IPM are drawn  
 166 randomly each year from some parametric statistical distributions. However, the exact  
 167 distribution from which the elements are taken is not defined *a priori* and will be  
 168 representative of the model species. The most common assumption is that time-varying kernel  
 169 elements are drawn independently from symmetric, Gaussian distributions, but it is possible

170 to use any other type of multivariate parametric statistical distribution (Rees and Ellner 2009).

171 The dynamics of the expected population size at time  $t+1$  given population size at time  
 172  $t$  can be written as:

$$173 \quad E[N(t+1)|N(t)] = \int_{\Omega} \int_{\Omega} \bar{k}(y, x) N(x, t) dx dy \quad (3)$$

174 where  $\bar{k}(y, x)$  is the mean kernel defined by averaging the stochastic kernel over all possible  
 175 environmental state values. Similar to equation (1), this dynamics is characterised by an  
 176 expected growth rate  $\bar{\lambda}$ , the stable state structure  $\bar{u}(x)$  and the reproductive value  $\bar{v}(x)$ . The  
 177 total reproductive value of the population can then be defined as  $V = \int \bar{v}(x) N(x)$ , which  
 178 equals total population size only when the population has the exact stable state structure. The  
 179 instantaneous rate of increase of the total reproductive value is then given by

$$180 \quad \Lambda_t = \frac{V_{t+1}}{V_t} = \bar{\lambda} + E_t + D \quad (4)$$

181 where  $E_t$  and  $D$  are random variables describing environmental stochasticity (i.e.,  
 182 between-year deviation from the mean kernel of the average individual contribution to total  
 183 reproductive value) and demographic stochasticity (i.e., within-year deviation from the mean  
 184 of the year of the individual contribution to total reproductive value), respectively (Engen et  
 185 al. 2007; Vindenes et al. 2011). Assuming no covariance between demographic and  
 186 environmental stochasticity, the variance in the instantaneous growth rate can be written as

$$187 \quad \text{Var}(\Lambda_t | V_t) = \text{Var}(E_t | V_t) + \text{Var}(D | V_t) = \sigma_e^2 + \sigma_d^2/V_t \quad (5)$$

188 for the case of a structured population model, including the IPM (Engen et al. 2007; Lande et  
 189 al. 2003; Vindenes et al. 2011). In equation (5),  $\sigma_e^2$  and  $\sigma_d^2$  are the environmental and  
 190 demographic variances, respectively. According to equation (5), the contribution of  
 191 demographic stochasticity depends on the demographic variance  $\sigma_d^2$  and is inversely  
 192 proportional to the total reproductive value.

193 An important property of a stochastic IPM is the long-run logarithmic growth rate,  
 194 denoted  $\ln \lambda_s$ , which describes the asymptotic exponential growth rate of the population size  
 195 after a sufficiently long time (Lande et al. 2003; Rees and Ellner 2009; Tuljapurkar 1990). For  
 196 a structured population, this long-run growth rate is best described by the dynamics of the  
 197 total reproductive value, which is Markovian, obeys a first-order autoregressive process, and  
 198 grows exponentially according to the same long-run growth rate as population size (Engen et  
 199 al. 2007; Engen et al. 2005). The long-run logarithmic growth rate can be approximated  
 200 assuming a small environmental noise, which implies that the population stays close to its  
 201 stable distribution (e.g., for IPM Rees and Ellner 2009). Following earlier work on  
 202 age-structured populations (Engen et al. 2007), Vindenes et al. (2011) showed that the  
 203 first-order approximation of the long-run growth rate of the stochastic IPM writes like

$$204 \quad \ln \lambda_s \approx \ln \bar{\lambda} - \frac{\sigma_e^2}{2\bar{\lambda}^2} - \frac{\sigma_d^2}{2\bar{\lambda}^2 V}, \quad (6)$$

205 where  $\bar{\lambda}$  is the deterministic population growth rate of the mean kernel.

### 206 Calculation of environmental and demographic variances

207 The demographic variance  $\sigma_d^2$  from equation (5) is given by the first-order approximation:

$$208 \quad \sigma_d^2 \approx \int_{\Omega} \bar{u}(y) \sigma_d^2(y) dy, \quad (7)$$

209 where the demographic variance due to an individual with trait value  $y$ , called  $\sigma_d^2(y)$ , is  
 210 weighted by the stable state structure  $\bar{u}(y)$  calculated for the mean kernel. Based on the work  
 211 by Vindenes et al. (2011), the term  $\sigma_d^2(y)$  can be further computed by using the expectation  
 212 of the demographic variance over all environmental states and a decomposition of the  
 213 individual contribution to total reproductive value, such that

$$214 \quad \sigma_d^2(y) = \underbrace{\bar{s}(y) \bar{\sigma}_{vs}^2(y)}_{\text{Growth variance}} + \underbrace{\bar{b}(y) \bar{\sigma}_{vb}^2(y)}_{\text{Offspringsize variance}} + \underbrace{\bar{\mu}_{vs}^2(y) \bar{\sigma}_s^2(y)}_{\text{Survival variance}}$$

## Viability analysis of size-structured populations

$$215 \quad + \frac{\overline{\mu_{vb}^2}(y)\overline{\sigma_B^2}(y)}{\text{Fecundity variance}} + \frac{2\overline{\sigma_{BS}^2}(y)\overline{\mu_{vs}}(y)\overline{\mu_{vb}}(y)}{\text{Survival-Fecundity covariance}} \quad (8)$$

216 All terms in equation (8) involve mean values over environments. They are precisely defined  
 217 in Appendix A, where we describe methods to estimate them. The three first variances can be  
 218 computed numerically from the model parameters and the reproductive value. The fecundity  
 219 variance depends on properties of the fecundity probability distribution, while the  
 220 survival-fecundity covariance is influenced by structural details of the model. For example, if  
 221 demographic census occurs after reproduction, reproduction is conditional on the survival of  
 222 parents, which implies a positive covariance between survival and fecundity.

223 In addition, the environmental variance is given by the first-order approximation:

$$224 \quad \sigma_e^2 \approx \int_{\Omega} \int_{\Omega} \overline{u}(x)\overline{u}(y)c(x, y)dxdy, \quad (9)$$

225 where  $c(x, y) = \text{cov}(E[W_x|Z], E[W_y|Z])$  is the covariance of expected contribution of  
 226 individual of trait value  $x$  ( $W_x$ ) and trait value  $y$  ( $W_y$ ) to the total reproductive value  
 227 (Vindenes et al. 2011). A first order approximation of the environmental variance can be  
 228 computed by calculating the variance in the population growth rate  $\lambda(z)$  with respect to the  
 229 environment state value  $z$  using stochastic simulations of large populations. Here, we  
 230 computed the asymptotic population growth rate  $\lambda(z)$  for 10,000 environments taken  
 231 randomly from the empirical probability distribution.

### 232 **Simulation of the IPM for finite populations**

233 We used an individual based, numerical version of the IPM (IBM) to simulate the stochastic  
 234 IPM for finite populations. The IBM included random, sampling variation for growth,  
 235 survival and reproduction according to the empirical distribution laws. We also parameterised  
 236 a diffusion approximation of the IBM following Vindenes *et al.* (2011), where the stochastic  
 237 discrete time dynamics is approximated by a continuous time Wiener process with drift,  
 238 which is entirely described by a drift term and an infinitesimal variance term (Lande and

239 Orzack 1988). We used the diffusion approximation to model the natural logarithm of the  
240 total reproductive value (Engen et al. 2005). The drift term is equivalent to the average  
241 logarithm of the stochastic growth rate from equation (6), while the variance term depends on  
242 the deterministic growth rate and the environmental and demographic variances (see  
243 Appendix B for detailed justification).

244 We simulated 50,000 runs of the IBM all starting from a reproductive value of 100  
245 and from the same state structure calculated from the stable state structure of the mean kernel.  
246 We calculated the instantaneous growth rate at each time step ( $\Lambda_t$  in equation (4)) and used  
247 all simulated trajectories to quantify the sample mean and sample variance of the growth rate  
248 from time  $t$  to time  $t+1$  given the reproductive value at time  $t$ . The diffusion approximation  
249 was simulated with the Matlab's econometry toolbox starting from a reproductive value of  
250 100. Similar qualitative results were obtained starting from a smaller or a larger population  
251 size. We calculated cumulative quasi-extinction risk during the first 50 years of the  
252 simulation, a reasonable time horizon for a PVA, with three quasi-extinction thresholds ( $N=1$   
253 equivalent to true extinction,  $N=10$ , and  $N=50$ ). We also calculated the cumulative extinction  
254 risk according to a previously published analytical expression that uses a diffusion  
255 approximation without demographic variance (Lande and Orzack 1988). We called this  
256 approximation the "large population analytical approximation" below (see equation (B10) in  
257 Appendix B for details). By comparing this analytical expression with results from the IBM  
258 and diffusion approximation of the IPM, it is thus possible to quantify the effects of  
259 demographic stochasticity on extinction risks.

### 260 **Prospective perturbation analyses**

261 Tools for the prospective analysis of IPM in response to small perturbations of the kernel  
262 include the deterministic elasticity (relative change of the deterministic growth rate  $\lambda$ ) and  
263 the stochastic elasticity (relative change of the long-run stochastic growth rate defined by

264 equation 3) to the mean and variance for kernel elements, parameters and functions  
 265 (Easterling et al. 2000; Rees and Ellner 2009). Here, we calculated only the deterministic  
 266 elasticity and the elasticity of the demographic variance constant  $\sigma_d^2$ , which are crucial to  
 267 PVA (Mills and Lindberg 2002). For the former, we calculated both (1) the elasticity surface  
 268 of  $\lambda$  to changes in the kernel, given by the relative sensitivity of  $\lambda$  to changes in the  
 269 function  $k(y, x)$  in a small area around  $y$  and  $x$ , and (2) the elasticity of  $\lambda$  to functions  
 270 of the kernel and model parameters (Easterling et al. 2000). We also evaluated the relative  
 271 impact of small changes in each parameter value on the demographic variance constant  
 272 defined in equation (5). This was done numerically through a slight (1%) perturbation of the  
 273 initial model. Because some parameter values were negative, we scaled sensitivities relative  
 274 to the absolute value of each parameter to obtain meaningful estimates.

### 275 **Case studies**

276 We gathered life history data for one plant species characterised by a life cycle structured by  
 277 height (redsepal evening primrose, *Oenothera glazioviana*) and one animal species  
 278 characterised by a life cycle structured by body size (common lizard, *Zootoca vivipara*). The  
 279 primrose population did not include estimates of environmental variance and was already  
 280 studied with a deterministic IPM by Rees and Rose (Rees and Rose 2002). Both IPM included  
 281 an annual census of the female portion of the population and were parameterised with life  
 282 history data collected inside one reference population for each species. Detailed information  
 283 on life cycles and model parameters is provided in Appendix C.

284 We first characterised all components of the stochastic growth rate in each study  
 285 species, and conducted the elasticity analyses and numerical simulations of finite populations.  
 286 In the case of the primrose model, further simulations were done where we tested different  
 287 parameter values for the seed mortality rate and the residual variation (standard deviation of  
 288 the random noise) of the growth function, which allowed us to test situations of decreasing,

289 almost stable and increasing populations with distinct patterns of deterministic growth and  
290 demographic variation (see Appendix C). The primrose model was chosen to do this analysis  
291 because it is simpler. In all models, we checked that our definition of the trait space did not  
292 bias the model outcomes through eviction of individuals near size limits (Merow et al. 2014).  
293 To do so, we calculated the size-dependent fraction eviction from the IPM conditional on  
294 survival and the unconditional fraction using equation (2) in Williams et al. (2012). The  
295 magnitude of eviction was negligible, even in the case of the primrose where size growth was  
296 linear with a high variance (e.g., less than 1% and 0.001% for unconditional and conditional  
297 fractions, respectively), and the fraction of evicted individuals was not influenced by changes  
298 in model parameters.

## 299 **Results**

### 300 **General characteristics of IPM**

301 Deterministic predictions for the growth rate (Table 1) and for the stable size structure (not  
302 shown) were similar to previously published observations. The primrose had an increasing  
303 population (+5% annual increase) in accordance with Rees and Rose (2002). The common  
304 lizard population displayed a local annual decrease of 10% in line with previous estimations  
305 from MPM (Le Galliard et al. 2010) and direct estimates of local recruitment and immigration  
306 (Lepetz et al. 2009). An analytical expression of each term in equation (8) made it possible to  
307 compute  $\sigma_d^2(y)$  using equation (7) and demographic variance using equation (6). The  
308 primrose population was characterised by the strongest demographic variance (see Table 1).  
309 In the common lizard, environmental variance was significant, since according to equation  
310 (6), the population size where demographic variance equals environmental variance is around  
311 20 individuals. A decomposition of the demographic variance according to size and the five  
312 variance terms in equation (8) showed that most demographic stochasticity was due to body  
313 growth and survival of adults while fecundity had little effects in the primrose (Figure 1a). A

314 strong negative correlation between fecundity and survival was observed. In the common  
315 lizard (Figure 1b), body growth had little influence on the demographic variance, which was  
316 almost entirely due to survival and fecundity.

### 317 **Elasticity analysis**

318 Elasticity surfaces represent the relative sensitivities of the deterministic growth rate to  
319 changes in the kernel. For the primrose (Figure 2a), the elasticity surface indicates the  
320 dominance of one size-specific transition, corresponding to transition of individuals into the  
321 reproductive stage, relative to two size-specific transitions of equal importance corresponding  
322 to growth of immature plants and offspring production. For the common lizard (Figure 2b),  
323 three size-specific transitions of equal relative importance were identified: survival and  
324 growth of juveniles, survival and growth of older individuals, and offspring production. We  
325 further calculated the elasticity of the growth rate ( $\lambda$ ) and demographic variance ( $\sigma_d^2$ ) for  
326 parameters in the primrose and lizard models (see Appendix E). In the primrose, elasticity of  
327  $\lambda$  was strongest for fecundity slope (measuring the increase of fecundity with rosette size),  
328 growth intercept (measuring mean rosette size early in life) and growth slope (measuring size  
329 increment per unit size at time  $t$ ), followed by survival intercept (measuring mean survival  
330 early in life). In the common lizard, fecundity and growth parameters had the strongest  
331 influence followed by juvenile survival, and adult survival had a weak influence. The  
332 elasticity of  $\lambda$  to change in one model parameter was positively correlated with the  
333 elasticity of  $\sigma_d^2$  to change in the same model parameter (Figure 2c).

### 334 **Population dynamics and extinction trajectories**

335 In the case of the common lizard, population dynamics predicted by the diffusion model fitted  
336 extremely well those observed in the IBM. This very good fit was observed throughout 50  
337 years of simulation in this case (see Figure 3a), but held over longer times with different  
338 initial conditions (results not shown). The relationship between the stochastic growth rate  $\Lambda_t$

## Viability analysis of size-structured populations

339 and population reproductive value predicted by the diffusion model was coherent with the one  
340 observed in the IBM or the one predicted by equation (6), except in very small populations  
341 where the diffusion approximation under-estimated the median and range of variation of the  
342 stochastic growth rate distribution of the IBM (Figure 3b). In this species, the diffusion  
343 approximation thus under-estimated slightly the variance of stochastic growth rate in very  
344 small populations (Figure 3c), where the probability distribution of the stochastic growth rate  
345 from the IBM did not fit the log-normal distribution assumed by the diffusion model (Figure  
346 3d).

347         Despite these small biases at very small population sizes, the cumulative  
348 quasi-extinction risk curves in the common lizard were very well predicted by the diffusion  
349 model even at low quasi-extinction thresholds (relative difference less than 5%, Figure 4a).  
350 Starting from ca. 100 individuals, this population had declining trends and characteristics  
351 quasi-extinction times of less than 50 years very well matched by the diffusion  
352 approximation. In the primrose population with positive growth, the risk of extinction was on  
353 average very small (ultimate quasi-extinction risk of less than 10%) and we identified a  
354 difference between predictions from the diffusion approximation and simulations of the IBM  
355 (relative difference more than 5%, Figure 4b). In this species, rare extinctions were caused by  
356 random events of rapid initial decline and demographic variance was very high due to  
357 stochastic variation in plant size. In this situation, the stochastic trajectories are likely to be  
358 more poorly captured by the diffusion approximation. In addition, as expected, differences  
359 between the diffusion approximation and the large population analytical approximation were  
360 higher at lower quasi-extinction thresholds in the lizard, i.e., when effects of demographic  
361 stochasticity on extinction times were stronger (Figure 4a).

362         In the primrose, increased parameter values for seed establishment probabilities and  
363 growth rate residual variance were associated with higher deterministic growth rate but also

364 higher demographic variance (see Table C1b in Appendix C), with a net negative effect on  
365 extinction risk. An analysis of the relative difference between quasi-extinction curves  
366 predicted by the diffusion approximation and those observed in the IBM revealed stronger  
367 biases during transient dynamics (intermediate simulation times) and when populations were  
368 less at risk of extinction (Fig. 5a, b). In all cases, the diffusion approximation under-estimated  
369 time to extinction and it also under-estimated the total cumulative risk of extinction for  
370 populations with positive intrinsic growth. To unravel if these biases were associated with  
371 differences in the characteristic dynamics of the populations or systematic failure to capture  
372 the properties of very small populations like in the common lizard, we plotted the bias for  
373 stochastic growth rate against population reproductive value. The results strongly suggested  
374 that this bias depended on population size irrespective of the model parameter values (Fig. 5c,  
375 d). The diffusion approximation systematically over-estimated the mean stochastic growth  
376 rate of the IBM in very small populations (less than 10-20 individuals).

### 377 **Discussion**

378 Until recently, the analysis of stochastic, size-structured populations rested essentially on  
379 individual based or matrix population models (Easterling et al. 2000; Enright et al. 1995;  
380 Pfister and Stevens 2003; Ramula et al. 2009). Here, we applied a new mathematical  
381 framework (Vindenes et al. 2011) designed specifically for small, size-structured populations  
382 and including both environmental and demographic variation. We performed basic population  
383 viability analyses, evaluated the model's accuracy in two species characterised by contrasted  
384 life cycles, and tested robustness of the model's predictions to changes in some model  
385 parameters in one model species. We found three results: (1) the extended IPM allows to  
386 decompose demographic variance to gain insights into most important size classes and  
387 demographic components, (2) the diffusion model with three parameters provided in general a  
388 very good approximation of the transient stochastic dynamics and ultimate extinction risks,

389 but (3) the diffusion approximation produced model-dependent biased estimates of the  
390 stochastic growth in very small populations.

### 391 **Model construction**

392 Given the number of tools available to conduct a PVA (Beissinger and McCullough 2002),  
393 one must be fully aware of the opportunities and constraints of the stochastic IPM. The kernel  
394 construction and parameter estimation are the most critical steps of the construction of an  
395 IPM. The kernel includes functions for growth, survival and reproduction. For our case  
396 studies, growth and reproduction functions and their yearly variation could be estimated  
397 relatively easily with regression techniques (Easterling et al. 2000; Rees and Ellner 2009).  
398 However, an accurate estimation of the survival function was more difficult to obtain for the  
399 lizard population since not all animals could be sampled. Thus, we used  
400 capture-mark-recapture models for closed populations, a procedure that can under-estimate  
401 true survival (animals can be lost due to movement outside the study site) and that makes it  
402 more difficult to assess size-dependent survival than standard logistic regressions (but see  
403 Frederiksen et al. 2013). In rare or declining species of conservation concern, accurate  
404 repeated censuses of the same population through time and a reasonable sample of individual  
405 records of one or two traits (e.g., body size) are therefore critical to parameterize the IPM and  
406 conduct a PVA (Ramula et al. 2009). For example, we have found it possible to parameterize  
407 an IPM for the critically endangered meadow viper with individual records of body size and  
408 reproduction in a very small population (less than 50 individuals, unpub. data).

409         Anyone willing to develop a stochastic IPM will also face three other difficulties.  
410 First, even if IPM provide more accurate estimates of  $\lambda$  than MPM for small data sets  
411 (Ramula et al. 2009), uncertainty in parameter values may lead to uncertainty in model  
412 predictions. Confidence intervals for model predictions could be obtained using Monte Carlo  
413 simulations or bootstrap re-sampling (McGowan et al. 2011). Second, the regression models

414 used to parameterize the IPM assumed small and normally distributed inter-annual variation.  
415 This assumption was backed up by long term data from the field, but other species may be  
416 characterised by catastrophic variation in survival (Baron et al. 2010). Individual-based  
417 simulations could be used to test the demographic consequences of such catastrophic  
418 variation. Third, a good knowledge of the probability distribution of kernel functions is  
419 required to model demographic stochasticity. We used binomial distribution for survival and  
420 Gaussian distribution for growth, but had no a priori expectation for the probability  
421 distribution of fecundity. In the common lizard, the generalized Poisson distribution was the  
422 best fit for the data because sample values were truncated at zero and had a clear upper bound  
423 (Kendall and Wittmann 2010).

#### 424 **Stochastic growth rate calculation**

425 The diffusion approximation and variance decomposition made it possible to describe  
426 stochastic dynamic with only three parameters (Vindenes et al. 2011): deterministic growth  
427 rate ( $\lambda$ ), demographic variance ( $\sigma_d^2$ ) and environmental variance ( $\sigma_e^2$ ). This decomposition  
428 provides a very powerful tool to assess the conservation status and compare the demography  
429 of size-structured species. The primrose population was characterised by a strong  
430 size-dependent demography and very high demographic stochasticity. The small demographic  
431 stochasticity in the common lizard dominated environmental variance only in populations of  
432 less than 20 individuals; thus, stochastic population dynamics were mainly driven by  
433 inter-annual effects similar to previous studies (Le Galliard et al. 2010). We anticipate that  
434 quantitative estimates of demographic and stochastic variance could be obtained in other  
435 size-structured species of plants and animals. Their comparison would be extremely useful to  
436 understand the relationship between stochastic population dynamics and life history similar to  
437 what was done with stage-structured animal populations (Saether et al. 2013).

438 A good understanding of demographic stochasticity is particularly relevant in

439 conservation biology. Here, we proposed a graphical approach to decompose the demographic  
440 variance which requires an analytical expression. This decomposition indicated that  
441 demographic variance was mostly due to growth variation for the primrose but survival  
442 variation in yearlings and adults for the common lizard. That plant growth contributed  
443 strongly to demographic variation in the primrose population may be due to the prolonged and  
444 weakly canalized compensatory growth trajectories. Plant growth lasted up to 10 years until  
445 maturation, and there was also a very high variability in growth rate (Kachi and Hirose 1983).  
446 In general, patterns of increasing size variability with age are common in plants because  
447 growth rates of individuals are often dependant and/or positively correlated through time  
448 (e.g., Pfister and Stevens 2002). The stochastic IPM would allow a better understanding of the  
449 effects of these complex growth strategies on demographic variance.

450         One important assumption made in the two case studies is that the life cycles are  
451 structured by one continuous covariate only. The framework of IPM also allows to include  
452 more than one continuous variable or a mixture of continuous and discrete state variables  
453 (Childs et al. 2003). To test the feasibility of this, we parameterised an additional IPM for the  
454 meadow viper (*Vipera ursinii ursinii*), an endangered species characterised by a complex life  
455 cycle structured by body size, age and breeding status (Baron et al. 2013; Ferrière et al. 1996).  
456 The combined size and stage structure was justified by the fact that maturation is conditional  
457 on the age (7 classes) and body size of immature females and because adult females alternate  
458 breeding and non-breeding years independent of their size (Baron et al. 2013). Unfortunately,  
459 the analytical expressions of the extended IPM were too cumbersome to allow a direct  
460 calculation and decomposition of the demographic stochasticity, and we had to rely on  
461 numerical simulations (results not shown). This difficulty could be encountered in many other  
462 species where demography is shaped by both continuous traits and discrete attributes such as  
463 stage, age, or habitat type (Ellner and Rees 2006). In such cases, we recommend to use the

464 IBM approach when the life cycle cannot be simplified without substantial loss of  
465 information, or to simplify the life cycle to a stage or age structured matrix population model.

466 **Elasticity analysis**

467 Prospective perturbation analysis of stochastic population dynamics include the calculation of  
468 many elasticities (this study, Easterling et al. 2000; Rees and Ellner 2009). In a real-life PVA,  
469 the conclusions of the elasticity analysis should be weighted by the feasibility and costs of all  
470 options available to improve the conservation status of the population. Here, we did not  
471 attempt to compute and compare all elasticities, but instead focused on the elasticity analysis  
472 of  $\lambda$  and  $\sigma_d^2$ . We found a positive correlation between elasticity for  $\lambda$  and for  $\sigma_d^2$ . Such  
473 correlations are expected whenever a management action to improve the mean of a trait also  
474 changes its variance, as is the case for the probability distributions of survival or fecundity.  
475 This correlation means that traits contributing more to deterministic growth may have lower  
476 effects on stochastic population growth than expected, especially at low population sizes.

477 The IPM is a useful tool for elasticity analysis of  $\lambda$  in a size-structured population  
478 because elasticities are not influenced by stage duration (Easterling et al. 2000). Elasticity  
479 surfaces indicate the most important size classes during a reintroduction or reinforcement  
480 program. In addition, the IPM allows to evaluate the elasticity to body growth and  
481 size-dependent demography, which is critical to the management of many important size  
482 structured populations such as hunted game species or marine fishes for example (Merow et  
483 al. 2014). Traditional PVA focuses on transition between stages (i.e., survival or migration)  
484 and fecundity, but tends to ignore body growth (Beissinger and McCullough 2002; Morris and  
485 Doak 2002). In life history theory, growth strategies are important because differences in  
486 body growth have implications for age and size at maturation, future fecundity and future  
487 survival. In addition, many species are characterised by plastic growth rates (French et al.  
488 2011; Gurnell et al. 2004). In the primrose and common lizard, the two parameters with the

489 highest elasticity for  $\lambda$  were the slope between fecundity and size and the basal size  
490 increment. Thus, conservation programs increasing body growth by improvement of habitat  
491 quality, removal of competitors, and food or nutrient supplementation should provide the  
492 most efficient management strategies in these species.

### 493 **Extinction dynamics**

494 Under the small noise approximation, Vindenes *et al.* (2011) constructed a diffusion model  
495 and demonstrated that this model fitted well the stochastic dynamics of one hypothetical  
496 stable size-structured population subject to demographic and environmental stochasticity. Our  
497 results obtained in two model species with contrasted life cycles, including one model species  
498 analysed with 25 different combinations of parameters, confirm these conclusions except in  
499 situations where the assumption of the small noise approximation is not met. We found that  
500 the diffusion approximation fitted very well the results of the stochastic IBM in intermediate  
501 and large populations (as a rule of thumb, when  $N > 20$ ), but tended to under-estimate or  
502 over-estimate the stochastic growth rate in very small populations. The direction of the bias  
503 was different in the two model species, and the impact of the bias was greater when  
504 populations had positive growth and thus extinction was not certain. According to our  
505 descriptive analyses, the differences were explained by a failure of the diffusion  
506 approximation to capture the probability distribution of the stochastic growth rate in very  
507 small populations.

508       Relatively few ecological studies have tested for sources of deviations between the  
509 diffusion approximation and the full stochastic model. It is expected that the diffusion  
510 approximation should fail when populations sizes are very small and growth variance  
511 becomes very large, especially in populations with large demographic variance such as the  
512 primrose. Engen *et al.* (2005) analysed a large number of age structured population models  
513 and found a reasonable fit in most cases, except for populations structured according to a

514 large number of age classes where the diffusion approximation could over-estimate the  
515 extinction risks. The case of density-dependent dynamics was investigated more  
516 systematically, and significant but relatively unpredictable model-dependent deviations were  
517 found (Kendall 2009; Wilcox and Possingham 2002). Wilcox and Possingham (2002) stated  
518 that such deviations could come from (1) inaccuracy in the estimation of the parameters of the  
519 diffusion approximation, (2) difficulties to capture unstable dynamics or rare events of  
520 population decline, and (3) unrealistic assumptions of the diffusion approximation. In our  
521 case, we included both demographic and environmental stochasticity in the diffusion  
522 approximation, and population dynamics were relatively smooth. Thus, the failure of the  
523 diffusion approximation at small population sizes was probably a consequence of the  
524 structural assumption of unbounded and normally distributed population growth rates (Lande  
525 et al. 2003; Ovaskainen and Meerson 2010). The magnitude of this bias will be difficult to  
526 predict because it seems to depend on the life cycle. Thus, we recommend to complement the  
527 extended IPM approach with individual based models to obtain unbiased estimates for very  
528 small populations of conservation concern.

529 **Acknowledgement:** We thank Manuel Massot and Jean Clobert for sharing field data. We  
530 thank Tom J.M. Van Dooren for comments that helped improved an earlier version of this  
531 manuscript. We are also grateful to the Parc national des Cévennes for providing access to the  
532 common lizard population. This research was supported by the Centre National de la  
533 Recherche Scientifique (CNRS), the Agence Nationale de la Recherche (ANR) program  
534 07-JCJC-0120, and the Région Ile-de-France R2DS program (grant 2007-06).

### 535 **References**

536 Baron J-P, Le Galliard J-F, Tully T, Ferrière R (2010) Cohort variation in offspring growth  
537 and survival: prenatal and postnatal factors in a late-maturing viviparous snake.  
538 *Journal of Animal Ecology* 79:640-649

## Viability analysis of size-structured populations

- 539 Baron J-P, Le Galliard J-F, Tully T, Ferrière R (2013) Intermittent breeding and the dynamics  
540 of resource allocation to growth, reproduction and survival. *Functional Ecology*  
541 27:173-183
- 542 Beissinger SR, McCullough DR (2002) *Population viability analysis*. The University of  
543 Chicago Press, Chicago, USA
- 544 Benton TG, Plaistow SJ, Coulson TN (2006) Complex population dynamics and complex  
545 causation: devils, details and demography. *Proceedings of the Royal Society of*  
546 *London B* 273:1173-1181
- 547 Caswell H (2001) *Matrix population models*. Sinauer Associates, Sunderland
- 548 Childs DZ, Rees M, Rose KE, Grubb PJ, Ellner SP (2003) Evolution of complex flowering  
549 strategies: an age- and size-structured integral projection model. *Proceedings of the*  
550 *Royal Society of London Series B-Biological Sciences* 270:1829-1838
- 551 Easterling MR, Ellner SP, Dixon PM (2000) Size-specific sensitivity: applying a new  
552 structured population model. *Ecology* 81:694-708
- 553 Ellner SP, Rees M (2006) Integral projection models for species with complex demography.  
554 *American Naturalist* 167:410-428
- 555 Engen S, Lande R, Saether BE, Festa-Bianchet M (2007) Using reproductive value to  
556 estimate key parameters in density-independent age-structured populations. *Journal of*  
557 *Theoretical Biology* 244:308-317
- 558 Engen S, Lande R, Saether BE, Weimerskirch H (2005) Extinction in relation to demographic  
559 and environmental stochasticity in age-structured models. *Mathematical Biosciences*  
560 195:210-227
- 561 Enright NJ, Franco M, Silvertown J (1995) Comparing plant life histories using elasticity  
562 analysis - the importance of life span and the number of life cycle stages. *Oecologia*  
563 104:79-84

## Viability analysis of size-structured populations

- 564 Ferrière R, Sarrazin F, Legendre S, Baron J-P (1996) Matrix population models applied to  
565 viability analysis and conservation: theory and practice with ULM software. *Acta*  
566 *Oecologica* 17:629-656
- 567 Frederiksen M, Lebreton J-D, Pradel R, Choquet R, Gimenez O (2013) Identifying links  
568 between vital rates and environment: a toolbox for the applied ecologist. *Journal of*  
569 *Applied Ecology* 51:71-81
- 570 French SS, Gonzalez-Suarez M, Young JK, Durham S, Gerber LR (2011) Human disturbance  
571 influences reproductive success and growth rate in California sea lions (*Zalophus*  
572 *californianus*). *PLoS ONE* 6
- 573 Gilpin ME, Soulé ME (1986) Minimum viable populations: processes of species extinction.  
574 In: Soulé ME (ed) *Conservation Biology: The science of scarcity and diversity*.  
575 Sinauer Associates, Inc. Publishers, University of Michigan, pp 19-34
- 576 Gross K, Morris WF, Wolosin MS, Doak DF (2006) Modeling vital rates improves estimation  
577 of population projection matrices. *Population Ecology* 48:79-89
- 578 Gurnell J, Wauters LA, Lurz PWW, Tosi G (2004) Alien species and interspecific  
579 competition: effects of introduced eastern grey squirrels on red squirrel population  
580 dynamics. *Journal of Animal Ecology* 73:26-35
- 581 Hughes JB, Daily GC, Ehrlich PR (1997) Population diversity: its extent and extinction.  
582 *Science* 278:689-692
- 583 Kachi N, Hirose T (1983) Bolting induction in *Oenothera erythrosepala* Borbás in relation to  
584 rosette size, vernalization, and photoperiod. *Oecologia* 60:6-9
- 585 Kendall BE (2009) The diffusion approximation overestimates the extinction risk for  
586 count-based PVA. *Conservation Letters* 2:216-225
- 587 Kendall BE, Fox GA (2002) Variation among individuals and reduced demographic  
588 stochasticity. *Conservation Biology* 16:109-116

## Viability analysis of size-structured populations

- 589 Kendall BE, Wittmann ME (2010) A stochastic model for annual reproductive success. *The*  
590 *American Naturalist* 175:461-468
- 591 Lande R, Engen S, Saether B-E (2003) Stochastic population dynamics in ecology and  
592 conservation. Oxford University Press, New York
- 593 Lande R, Orzack SH (1988) Extinction dynamics of age-structured populations in a  
594 fluctuating environment. *Proceedings of the National Academy of Sciences of the*  
595 *United States of America* 85:7418-7421
- 596 Le Galliard J-F, Marquis O, Massot M (2010) Cohort variation, climate effects and population  
597 dynamics in a short-lived lizard. *Journal of Animal Ecology* 79:1296-1307
- 598 Lepetz V, Massot M, Chaine A, Clobert J (2009) Climate warming and the evolution of  
599 morphotypes in a reptile. *Global Change Biology* 15:454-466
- 600 McGowan CP, Runge MC, Larson MA (2011) Incorporating parametric uncertainty into  
601 population viability analysis models. *Biological Conservation* 144:1400-1408
- 602 Merow C et al. (2014) Advancing population ecology with integral projection models: a  
603 practical guide. *Methods in Ecology and Evolution* 5:99-110
- 604 Mills LS, Lindberg MS (2002) Sensitivity analysis to evaluate the consequences of  
605 conservation actions. In: Beissinger SR, McCullough DR (eds) *Population Viability*  
606 *Analysis*. University of Chicago Press, Chicago, IL, pp 338-366
- 607 Morris WF, Doak DF (2002) *Quantitative conservation biology*. Sinauer Associates
- 608 Ovaskainen O, Meerson B (2010) Stochastic models of population extinction. *Trends in*  
609 *Ecology & Evolution* 25:643-652
- 610 Pfister CA, Stevens FR (2002) The genesis of size variability in plants and animals. *Ecology*  
611 83:59-72
- 612 Pfister CA, Stevens FR (2003) Individual variation and environmental stochasticity:  
613 Implications for matrix model predictions. *Ecology* 84:496-510

## Viability analysis of size-structured populations

- 614 Ramula S, Rees M, Buckley YM (2009) Integral projection models perform better for small  
615 demographic data sets than matrix population models: a case study of two perennial  
616 herbs. *Journal of Applied Ecology* 46:1048-1053
- 617 Rees M, Ellner SP (2009) Integral projection models for populations in temporally varying  
618 environments. *Ecological Monographs* 79:575-594
- 619 Rees M, Rose KE (2002) Evolution of flowering strategies in *Oenothera glazioviana*: an  
620 integral projection model approach. *Proceedings of the Royal Society of London*  
621 *Series B-Biological Sciences* 269:1509-1515
- 622 Saether B-E et al. (2013) How life history influences population dynamics in fluctuating  
623 environments. *The American Naturalist* 182:743-759
- 624 Tuljapurkar S (1990) *Population dynamics in variable environments*. Springer Verlag, Berlin,  
625 Germany
- 626 Vindenes Y, Engen S, Saether BE (2011) Integral projection models for finite populations in a  
627 stochastic environment. *Ecology* 92:1146-1156
- 628 Wilcox C, Possingham H (2002) Do life history traits affect the accuracy of diffusion  
629 approximations for mean time to extinction? *Ecological Applications* 12:1163-1179
- 630 Williams JL, Miller TEX, Ellner SP (2012) Avoiding unintentional eviction from integral  
631 projection models. *Ecology* 93:2008-2014
- 632
- 633
- 634

635 **Figure legends**

636 **Figure 1.** Decomposition of demographic variance according to size and demographic  
637 components in the primrose (a) and common lizard (b) after equation (9). The primrose model  
638 was structured by rosette size (mm, log scale) and the common lizard model was structured by  
639 body size (snout-vent length, mm). The areas of different colour indicate the relative  
640 contribution of each component to total demographic variance at a given size, including  
641 negative contributions.

642 **Figure 2.** Elasticity analysis of the deterministic growth rate and of the demographic variance.  
643 a-b. Elasticity surfaces of the deterministic growth rate  $\lambda$  with respect to the projection kernel  
644 of the primrose (a) and the common lizard (b). c. Elasticity of the demographic variance  
645 against elasticity of the deterministic growth rate  $\lambda$  with respect to the same model parameter  
646 for the common lizard (squares) and primrose (circles) models. Elasticity was calculated with  
647 respect to a small change in the value of each parameter describing size-dependent survival,  
648 growth and reproduction functions of the projection kernel (see Appendix D for raw data).

649 **Figure 3.** Comparison of the simulations of the diffusion approximation of the IPM  
650 (diffusion) with the simulations of the individual based model (IBM) and the predictions from  
651 the small-noise first order approximation (LPA) for the common lizard. a. Population  
652 trajectories (75% , 50% and 25% quantiles of the total reproductive value) predicted by the  
653 diffusion approximation and the IBM. b. Stochastic growth rate (mean and quantiles) against  
654 population reproductive value from the diffusion approximation, the IBM and the small-noise  
655 approximation of equation (6). c. Variance of the stochastic growth rate variance against  
656 inverse of population reproductive value from the diffusion, the IBM and the small-noise  
657 approximation of equation (6). For the diffusion approximation and the IBM, reproductive  
658 values and stochastic growth rate statistics were calculated from the simulations displayed in  
659 panel a. The inverse of the population reproductive value was used to ease visualization. d.

## Viability analysis of size-structured populations

660 Probability distributions of the stochastic population growth rate in small (20 individuals) and  
661 very small (5 individuals) populations from the diffusion approximation and the IBM. Similar  
662 qualitative results were obtained with the other models.

663 **Figure 4.** Cumulative extinction risks predicted by the diffusion approximation of the IPM  
664 (diffusion), the individual based model (IBM) and the large population analytical  
665 approximation (LPA) of Lande and Orzack (1988). The latter was not plotted in the primrose  
666 model because this model does not include environmental variation. Extinction probability  
667 was computed for a quasi-extinction threshold of 50 (black), 10 (grey) and 1 (light grey)  
668 individuals for the common lizard (a) and the primrose population (b). All simulations started  
669 from a reproductive value of 100. Note the difference in the y-axis range in panel (b) where  
670 population growth was positive and ultimate extinction risk is less than 1.

671 **Figure 5.** Sensitivity analysis of the quality of the IPM diffusion approximation in the  
672 primrose model. Relative difference between the cumulative quasi-extinction curves of the  
673 diffusion approximation of the IPM and those of the IBM with increasing values (from dark  
674 to light curves) of the seed establishment probability (a) and the residual variation (standard  
675 deviation) of the size growth (b). A negative relative difference indicates that the diffusion  
676 approximation tends to under-estimate the extinction probability. To understand the observed  
677 patterns, we calculated the relative difference between the mean stochastic growth rate of the  
678 diffusion approximation and of the IBM (c, d). Mean stochastic growth rate was calculated at  
679 each reproductive value reached by the simulations and curves were then smoothed with a  
680 moving average method to ease interpretation. Fluctuations come from small sample size of  
681 data to calculate extinction risk and biases between the diffusion approximation and IBM.  
682 Deterministic growth is higher than 1 when seed establishment probability  $< 0.008$  (panels  
683 a-c) and when growth residual variation  $< 0.3364$  (panels b-d).

684

## Viability analysis of size-structured populations

685 **Table 1**

686 Estimates of the asymptotic growth rate ( $\lambda$ ), demographic variance ( $\sigma_d^2$ ) and environmental  
687 variance ( $\sigma_e^2$ ) from equation (3). In the primrose, no estimate of environmental variance was  
688 available implying that estimate of demographic variance was probably inflated.

689

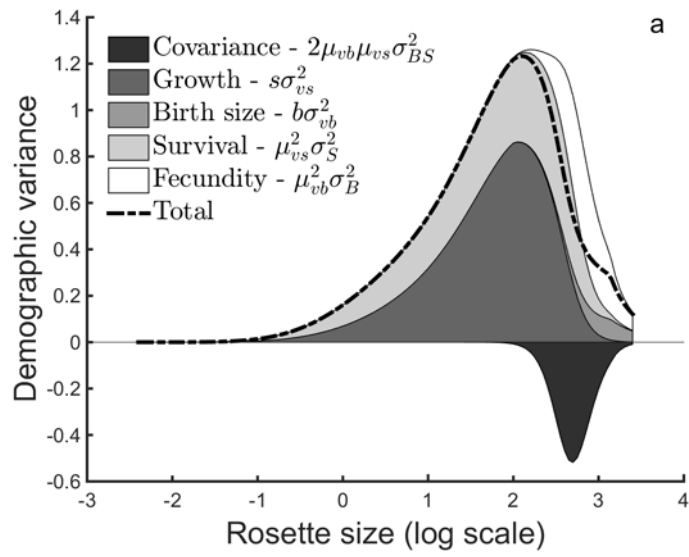
<i>Model</i>	$\lambda$	$\sigma_d^2$	$\sigma_e^2$
<i>Oenothera glazioviana</i> (primrose)	1.0526	2.2487	0
<i>Zootoca vivipara</i> (common lizard)	0.9077	0.4566	0.0204

690

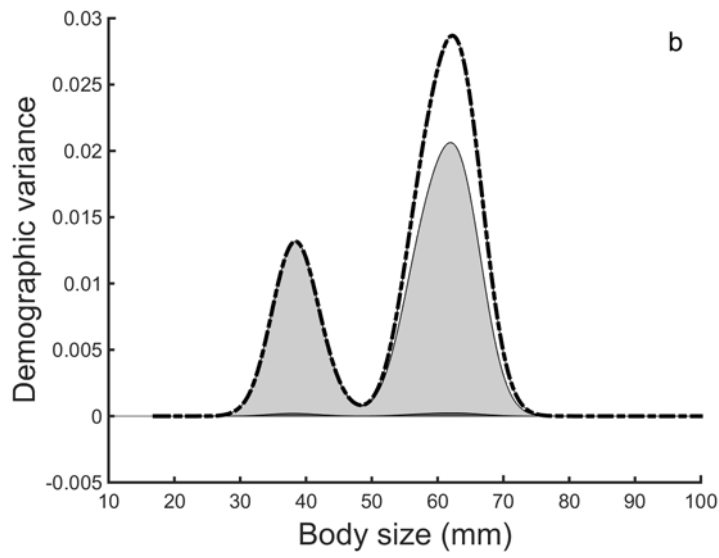
691

692 **Figure 1**

693



694

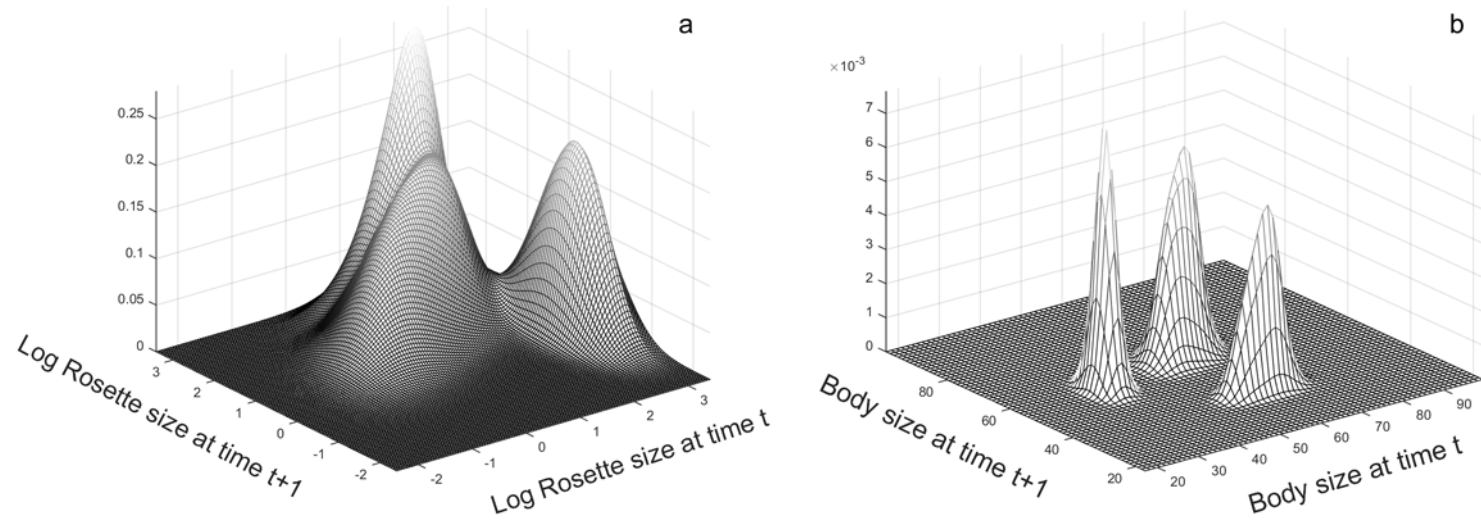


695

696

697 **Figure 2**

698

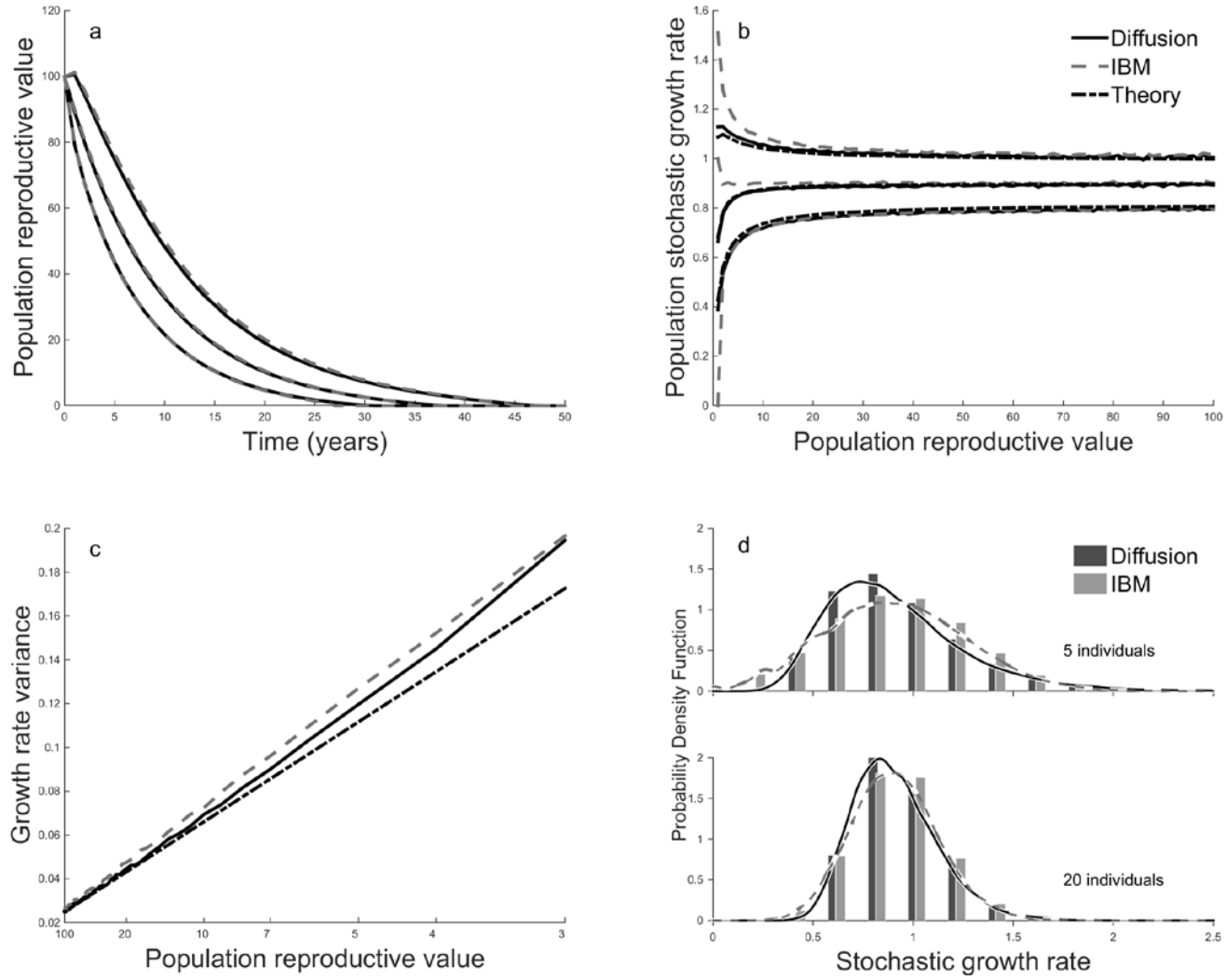


699

700

701

702 **Figure 3**

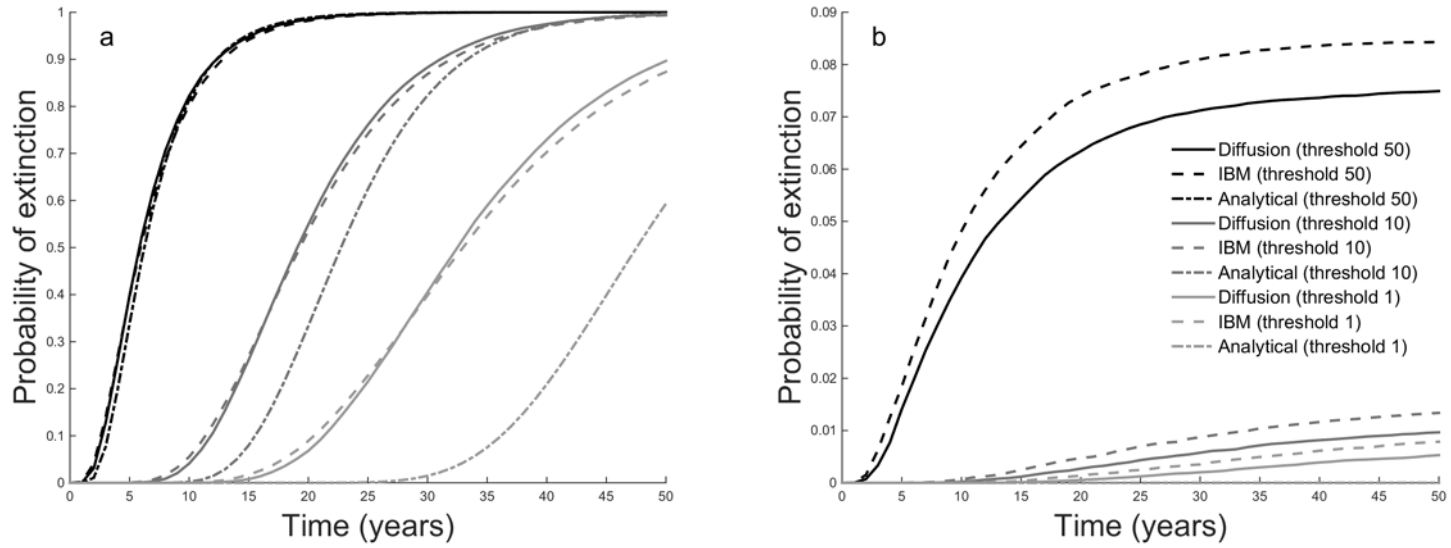


703

704

705

706 **Figure 4**



707

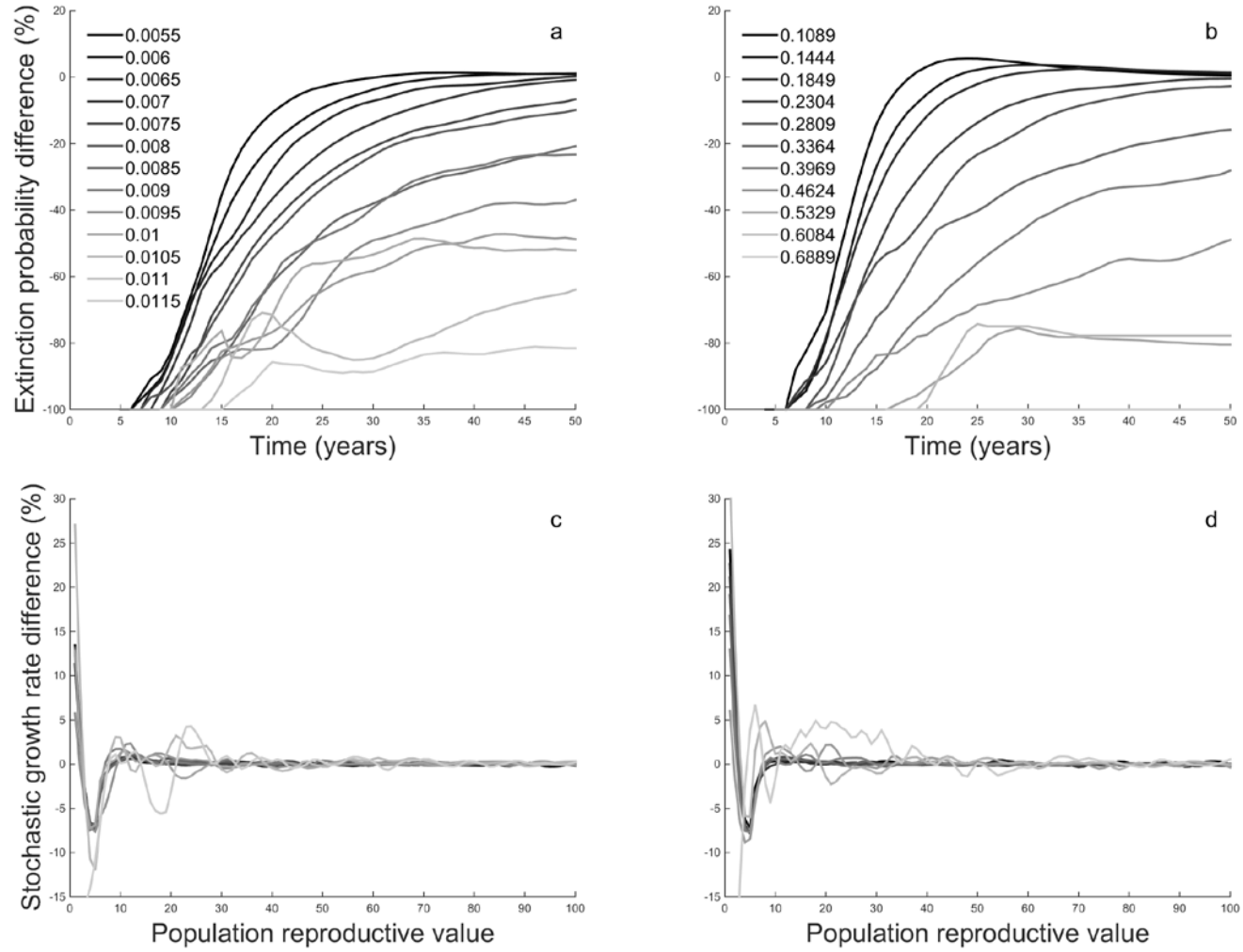
708

709

1 PA  
1 PA

Viability analysis of size-structured populations

710 **Figure 5**



711

712

713